Electrochemical Performance of Polyphosphonitrile Carbon Spheres as Anode Materials

Zhengping Zhao[1,2], Sitao Shen[2], Yuting Li[2], Mingqiang Zhong[2] and Jiawei Chew[3,]*

[1] Zhijiang College, Zhejiang University of Technology, Hangzhou 310014, China
[2] College of Materials Science and Engineering, Zhejiang University of Technology, Hangzhou 310014, China
[3] School of Chemical and Biomedical Engineering, Nanyang Technological University, 637459, Singapore
[*]E-mail: JChew@ntu.edu.sg

As a typical organic-inorganic hybrid material, polyphosphazene material has become popular in the field of porous carbon materials which can be used as electrode materials applying to super capacitors, lithium batteries and other energy storage device to obtain better electrochemical properties. Polyphosphazene microspheres covered with transition metal were prepared by a step of precipitation polymerization. Black powder is obtained after high temperature carbonization. The microstructure structures of the materials are analyzed by IR, Raman, SEM and TEM analysis technique. In the aspect of electrochemical performance, the results show that the obtained carbon materials have high specific capacitance and exhibits excellent stability. Cobalt disulfide carbon composites are a modification of the gauge mesoporous carbon materials. The carbon microspheres grow many layers of cobalt disulfide with a high specific surface area, good electrochemical performance and dimensional stability, which can be widely used in anode materials for lithium ion batteries. This experiment using polyphosphazene microspheres as carbon source, and direct hydrothermal synthesis of cobalt disulfide on the lignin surface, then through the pyrolysis made porous carbon materials. Finally, the electrochemical properties of the carbon materials were tested and analyzed. The purpose is to develop a kind of high performance lithium ion battery cathode material which can utilize polyphosphazene as carbon source.

1. INTRODUCTION

As a typical organic-inorganic hybrid material, polyphosphazene material has become popular in the field of materials research due to its comprehensive superior performance. Functional polyphosphazene micro-nano-materials, which is prepared by the nanotechnology combining

polyphosphazene material，possesses template self-assembled, precursor of carbonized mesoporous materials, and excellent design of molecular structure [1-4]. With these characteristics, it can be further prepared for porous carbon materials [5]. This composite porous carbon material, which is based on polyphosphazene carbon precursor, can be used as electrode material applying to super capacitors, lithium batteries and other energy storage device, also leads to better electrochemical properties [6-7]. Therefore, it has great research significance and application prospects.

The theoretical capacity of CoS_2 as a cathode material for li-ion batteries is very large, and it is a promising electrode material choice [8-11]. However, when CoS_2 is used as electrode material alone, the insertion process of lithium ions will lead to the change of CoS_2 volume, so that its actual electrochemical performance is not very ideal. At present, the porous carbon materials is a good and practical use value of the electrode materials [12-15]. This paper assumes that the preparation of porous carbon materials coated CoS_2 of new composite material, through the channel of carbon material, in the guarantee for embedded lithium ion contact with CoS_2 and process to obtain a high capacity performance at the same time. The use of carbon materials good structural stability to avoid layered CoS_2 volume change, which is expected to get excellent cycle stability of CoS_2/carbon composites. In addition to further improve the electrochemical performance of the electrode material, this paper uses carbide mesoporous material before the body characteristics of functional micro/nano materials as carbon source. The functional micro/nano materials polyphosphonitrile with template self-assembly properties, making the coated CoS_2 has the possibility of implementation, and in the process of coating (based on the PZs) can form polyphosphonitrile micro ball, which can have a larger contact area with the electrolyte and improve the electrochemical properties. In addition, the molecular structure of polyphosphazenes can design and make it further modified strengthen space. The C-PZs/CoS_2 composite materials based on the polyphosphazene carbon precursor can be used as electrode material to further assemble the lithium battery. At present, CoS_2/carbon composites are mostly distributed on carbon materials, so the synthetic route proposed in this paper can enrich the preparation methods of the composites.

2. EXPERIMENTAL SECTION

2.1 Materials

Cobalt disulfide (CoS_2), Hexachlorocyclotriphosphazene (HCCP), 4,4'-dihydroxydiphenylsulfone (BPS), triethylamine (TEA), acetonitrile, acetylene black and polyvinylidene fluoride (PVDF) were all analytical reagents purchased from Shanghai Chemical Reagents Corp (Shanghai, China).

2.2 Preparation of carbon source materials

Quantitative hexachlorocyclotriphosphonitrile, 4,4'-dihydroxydiphenylsulfone and molybdenum disulfide ultrasound were dispersed in acetonitrile solvent, then triethylamine was added

by 500 W ultrasound for 5 h. Centrifugalized the solid material and washed by ethanol and deionized water for 3 times, respectively. And vacuum drying at 40 ℃ for 24 h to obtain the PZs@CoS$_2$ microspheres. To join the tube furnace, slow warming to 900 ℃ temperature for 1 h and then cooling to room temperature along with the furnace to obtain the C-PZs@CoS$_2$ carbon materials as the anode materials for lithium ion batteries. In additional, PZs and C-PZs carbon materials without CoS$_2$ were also prepared by the same method.

2.3 Characterization

FT-IR spectra of all samples were recorded using polymer granule on a Perkin-Elmer Wellesley MA spectrophotometer. Thermogravimetric analysis (TGA) was performed on a TGA 7 instrument (PerkinElmer) thermal analysis system. Sample weight taken was 2-4 mg. All the experiment data were taken as an average of at least five measurements. The microstructures were observed on a Hitachi S4000 Scanning Electron Microscope and a JEOL 200CX Transmission Electron Microscope. Raman spectroscopy is a method for qualitative analysis of molecular structure. The chemical structures were observed on a Lab RAM HR UV800 laser Raman spectrometer (JOBIN YVON, France). The excitation light source is 632.81 nm and the scanning range is 200~4000.

The constant charge-discharge performance was tested after the sample electrode material was assembled into CR 2025 button battery. The electrochemical performances such as power density, energy density and specific capacitance can be obtained by processing and analyzing the results of constant current charge-discharge test [16]. The calculation formula of specific capacitance is:

$$Cs = I\Delta t/m\Delta V \tag{1-1}$$

Where I(A) is the charge-discharge current. Δt for discharge time. m is the mass of the active substance in the electrode material. ΔV is the discharge voltage range.

The cyclic voltammetry is to discuss the reaction of capacitor electrode after applying triangular waveform potential. The applied control signal is potential, and the measured corresponding signal is current. It is mainly to study the change rules of I-t and I-U. The relation curve of U-I can be obtained by observing the T-t graph [17].

3. RESULTS AND DISCUSSION

Figure 1 shows the infrared spectrum of polyphosphonitrile microspheres (PZs). According to HCCP infrared spectrum, 1317, 1210, 1190 and 876 cm^{-1} are the characteristic peaks of HCCP (refer to [5]).
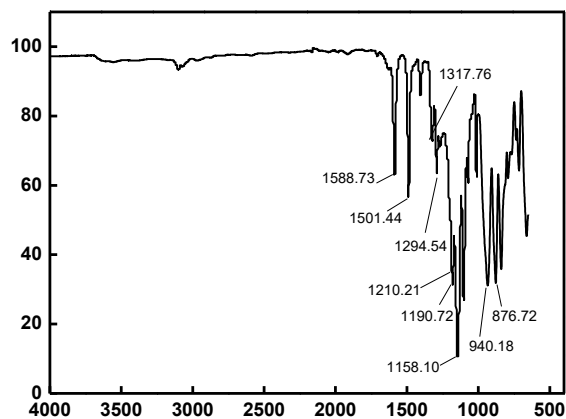
Figure 1. FTIR infrared spectrogram of PZs

In addition to the absorption peaks, figure 1 shows the absorption peaks of 1588 and 1501 cm^{-1} are derived from the phenyl unit of 4,4'-dihydroxydiphenylsulfone (BPS), which are the resonant absorption peaks of carbon-carbon double bonds (C=C(Ph)) in the benzene ring. There are two absorption peaks at 1294 cm^{-1} and 1158 cm^{-1} corresponding to the resonance absorption of the sulfone (O=S=O) in BPS. The phenolic hydroxyl absorption peaks (3000-3500 cm^{-1}) that should have existed in BPS were disappeared in figure, but the P-O-(Ph) resonance absorption peak appeared at 940 cm^{-1}, which can prove that HCCP and BPS have successfully performed condensation polymerization. The synthesis mechanism of PZs was identical to polyphosphazene derivatives [18]. The structure of it is characterized by a three dimension crosslinked network structure and there is a porous structure inside the resin.

Figure 2 and 3 show the thermal performance test results of PZs nano-microspheres and coated CoS$_2$ particles, respectively. From figure 2, the pyrolysis reaction of PZs microspheres is at the range of 478 to 546 °C temperature under N$_2$, and the residues is 54.2% continued to heat up to 800 °C. From figure 4, it is indicated that the pyrolysis reaction coated with CoS$_2$ is very severe within the temperature range of 440 to 476 °C and 821 to 851 °C, and the solid residue rate is 40.7% up to 900 °C. The reason is that small molecules and non-carbon components sublimate and escape at high temperature due to poor thermal stability, but the remaining carbon pellets are stable. Comparing the two microspheres TGA curves, the thermal stability of PZs microspheres coated with CoS$_2$ is slightly worse than that of non-coated, but the residual quantity is slightly lower. It is indicated that CoS$_2$ has certain influence on the thermal stability of PZs. According to the TGA curves, the high temperature carbonization process of PZs microspheres can also be obtained.
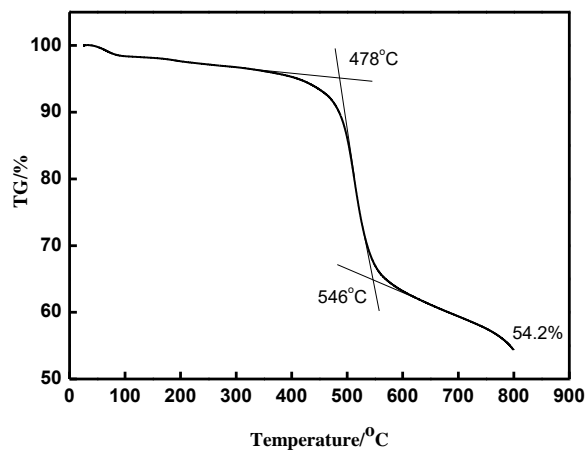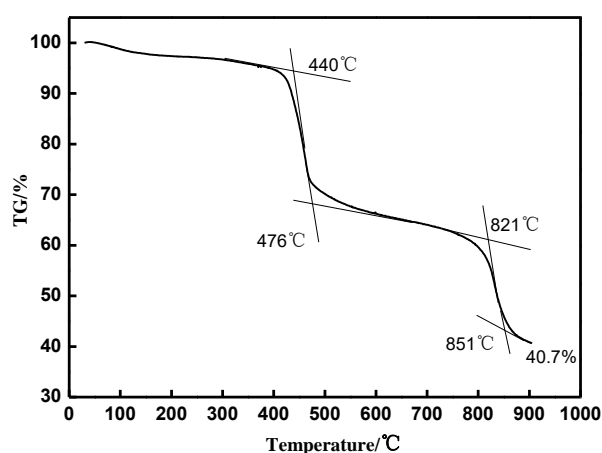
Figure 2. TG curve of PZs

Figure 3. TG curve of PZs@CoS$_2$

SEM shows that PZs microspheres were successfully synthesized by precipitation polymerization. It can be seen from figure 4 that the dispersion effects of PZs microspheres are very excellent under 500 w ultrasonic and the size of microspheres is relatively consistent. The size of the microsphere is 500 to 600 nm. Figure 4d shows that the material still remains microsphere after carbonization at high temperature, and a small part of the material is collapsing and the reason is that the low crosslinking density leads to further intramolecular and intermolecular reactions at high temperature. PZs microspheres were highly crosslinked. During the carbonization process, small molecules spilled out and the microsphere skeleton remained unchanged. The result is a polyphosphonitrile carbon sphere with a large number of pores were formed. Polyphosphazonitrile carbon spheres are rich in nitrogen and phosphorus atoms, which can improve the specific capacity of microspheres. The specific capacitance is higher than that of 372 mAh/g pure carbon material [19].
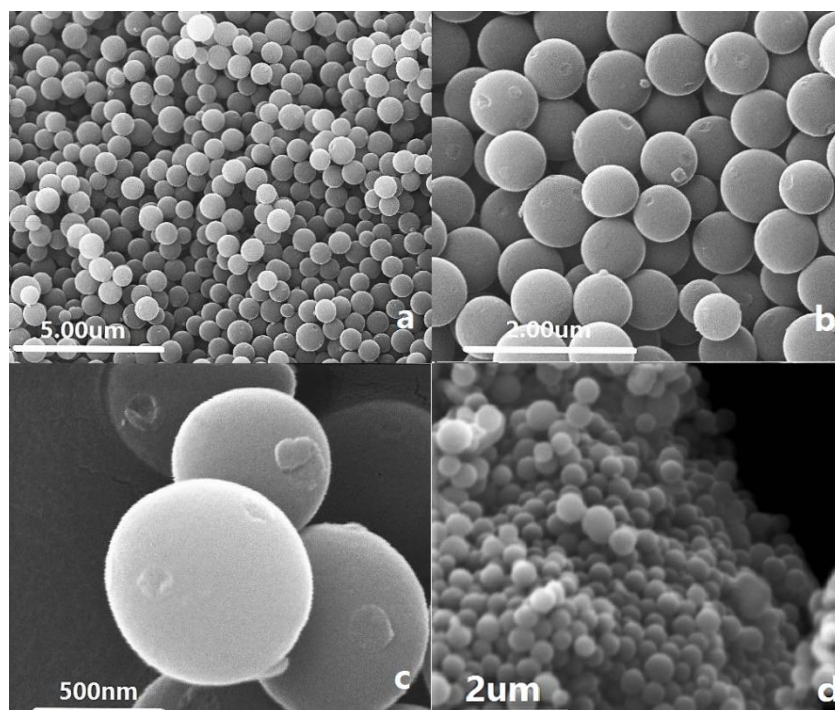
Figure 4. SEM images of PZs@CoS$_2$

Figure 5d and e are the TEM images of microspheres slices. It can be clearly seen that the coated structure and dispersion is well. Figure 5f is the black substance in figure 5e with further magnification, and obvious layered structures can be seen. The interlayer spacing is about 0.63 nm, which is close to the reference value (0.65 nm) [20]. TEM energy spectrum scanning also confirmed that the black materials are CoS$_2$. Therefore, the results show that PZs microspheres successfully coated CoS$_2$.

Raman spectroscopy also be used to characterize the different kinds and structures of carbon materials, and is also widely used to detect the degree of graphitization. G peak is derived from graphite carbon materials, and D peak refers to the disorder degree and defect of carbon materials. The purity of aromatic ring cluster can be obtained through the ratio ID/IG of the two peaks area, which is namely the degree of graphitization.

From figure 6, the location of D peak is 1348.37 cm^{-1}, the location of G peak is 1589.85 cm^{-1}, and ID/IG=1.16. The degree of graphitization of the materials obtained from the above data is relatively large, and these graphitized structures can facilitate electron transmission and facilitate the formation of electrode materials [21].
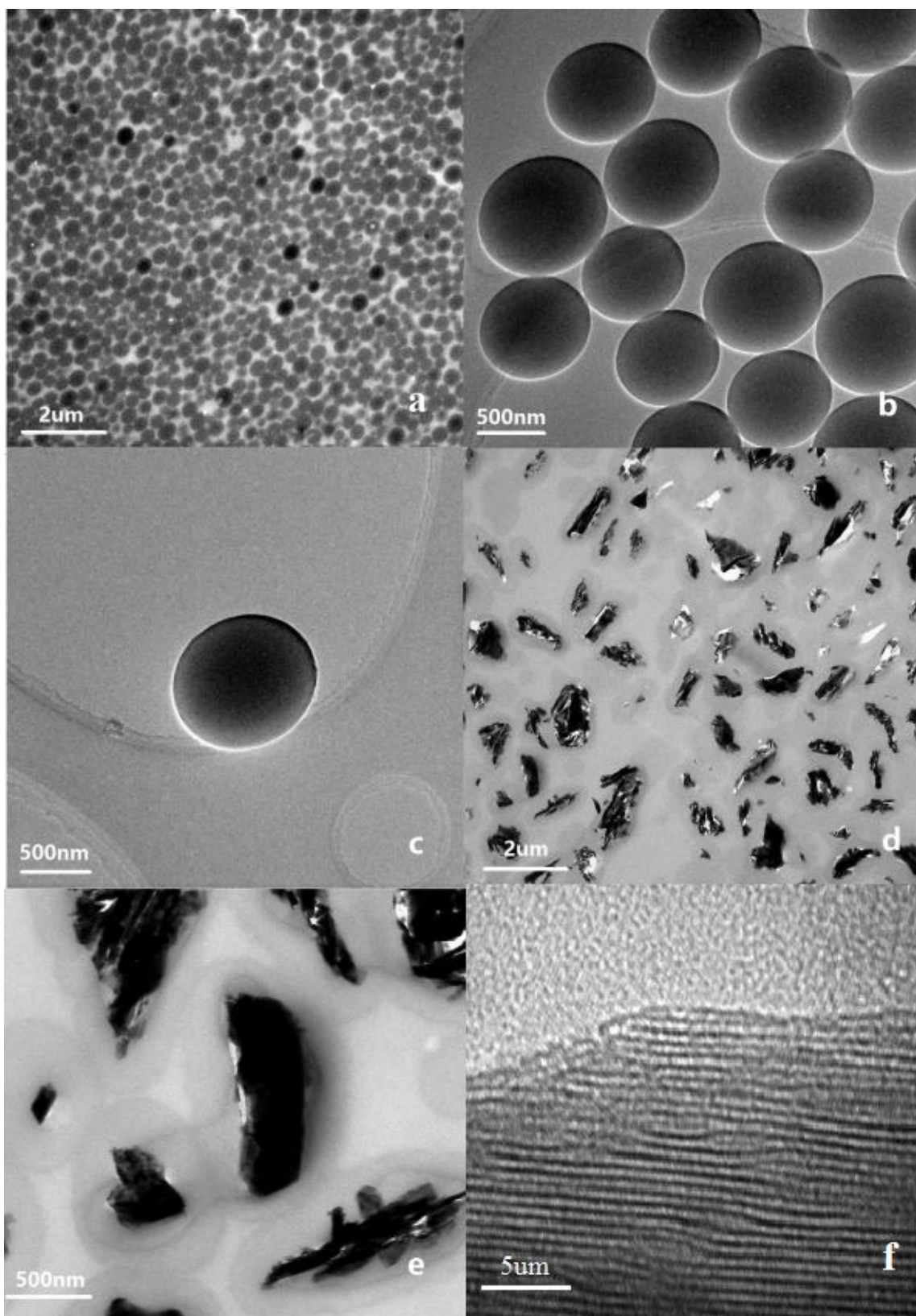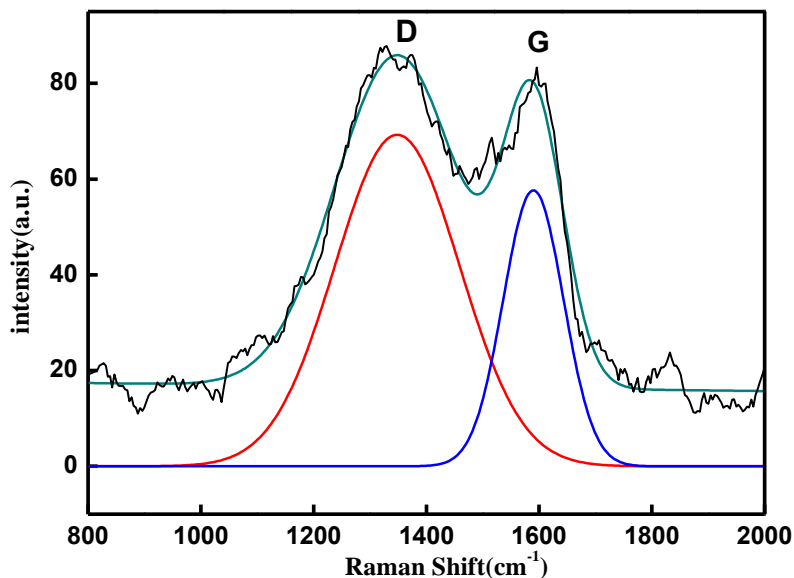
Figure 5. TEM images of PZs@CoS$_2$

Fugure 6. The Raman spectra of C-PZs@CoS$_2$

From the 50 charge-discharge curves of C-PZs and C-PZs@CoS$_2$, the first discharge ratio capacitance are 596 and 1080 mAh/g, respectively. But the charging capacity and discharge capacity of the two samples are close to each other, which indicating that the carbon material prepared has excellent reversible performance. Respectively contrast the 10th first charge-discharge capacity, C-PZs@CoS$_2$ has larger losses. It may because that the coated CoS$_2$ is less, which shows larger capacitance when CoS$_2$ began to contact the lithium ions and took place of embedded-slipped out reaction. But with repeated charging-discharging, CoS$_2$ had certain changes in the volume to cause its electrochemical performance degradation. From the specific capacitance of the two carbon balls, coated CoS$_2$ shows better electrochemical performance. The capacitance retention of C-PZs@CoS$_2$ sample is more stable. The high capacitive retention rate indicates that the material has larger specific surface area and pore structure, and the pore structure is not easy to collapse and deform, which can ensure Li$^+$ ions pass in and out [22].
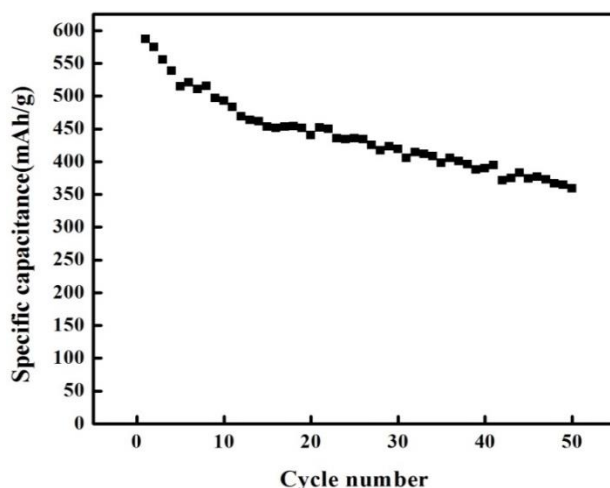

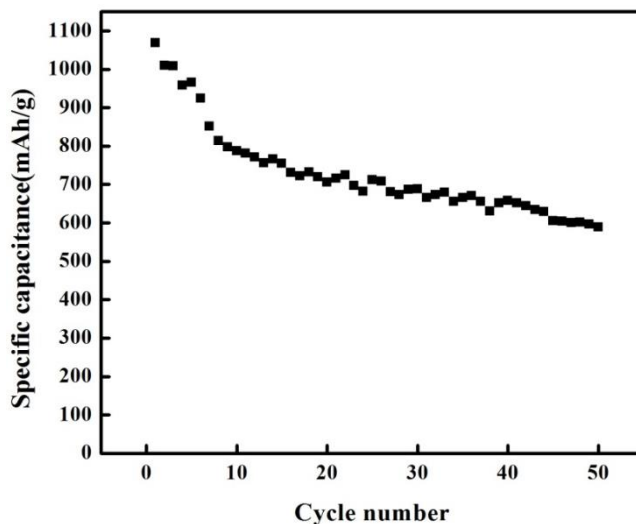**Figure 7.** The retention rate of specific capacitance of C-PZs

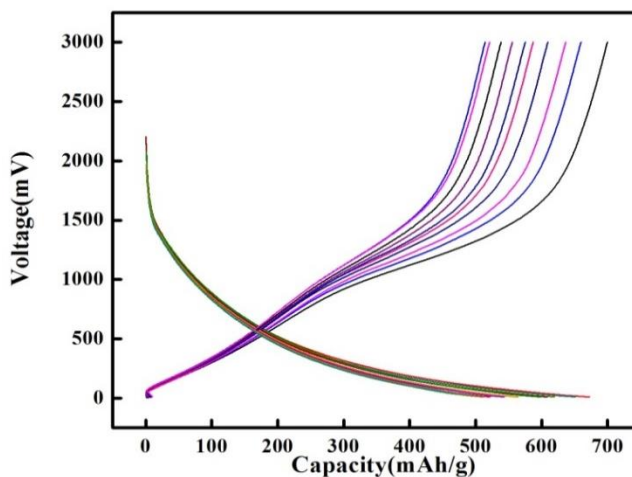**Figure 8.** The retention rate of specific capacitance of C-PZs@CoS$_2$

Figure 9. The first ten charge-discharge curves of C-PZs
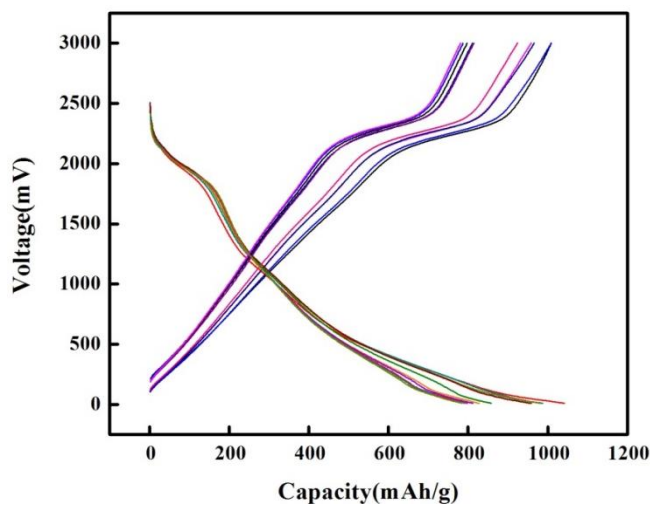

Figure 10. The retention rate of specific capacitance of C-PZs@CoS$_2$

The comparsion of C-PZs/CoS$_2$ and other anode materials were added in table 2.

Table 1. The capacity of anode materials

anode materials	capacity (mAh·g^{-1}, 100 cycles)	retention rate (%, 100 cycles)
petroleum carbon [2]	264	77.0
C-PZs/CoS$_2$	1089	73.5
NiO@carbon [5]	573	84.4
S@Li@carbon [16]	1294	87.8
Si@carbon [18]	3241	71.2

As can be seen from table 1, traditional petroleum carbon anode materials have a lower specific capacity and the corresponding 100 cycle retention rate is also low. It is also verified that only the embedding and stripping of lithium ions exist in the charging and discharging process of petroleum carbon anode materials. The specific capacity of the battery is also proportional to the graphitization degree of the carbon material. The higher the graphitization degree, the higher the specific capacity. However, its maximum specific capacity is 372 mAh·g^{-1}, which is much lower than the application of transition metal or metal oxide as anode material. Si has the highest specific capacity, which is 3241 mAh·g^{-1} after 100 charge and discharge cycles, but has the defect of large expansion coefficient. While the higher cycles, the reduction in specific capacity is more significant. It is mainly caused by the crushing of Si grains. Limited by the specific capacity of CoS$_2$ material itself, the materials listed in the table are in the middle. However, C-PZs/CoS$_2$ has the highest specific capacity retention rate. And the specific capacity is 4 times that of petroleum carbon, which has a high application value. Due to the influence of their conductivity or volume expansion, other transition metals or metal compounds need to be prepared with carbon materials as negative materials. However, these anode materials are all in the experimental research stage, but fewer are widely used. Therefore, there is still a long way before the real large-scale application, which requires new breakthroughs in structural design and manufacturing.

Figure 11 and 12 are the cyclic voltammetry (CV) curves and capacitance charts of C-PZs and C-PZs@CoS$_2$ at 0.1, 0.06, 0.04, 0.02, 0.01 and 0.005 v/s sweep rates, respectively. As can be seen from the schematic information, the CV curves are typical of the carbon material CV curve [23]. For the same sample, the absolute area of the cyclic voltammetry increases with the increase of sweep rate and the corresponding specific capacitance decreases with the increase of sweep rate.
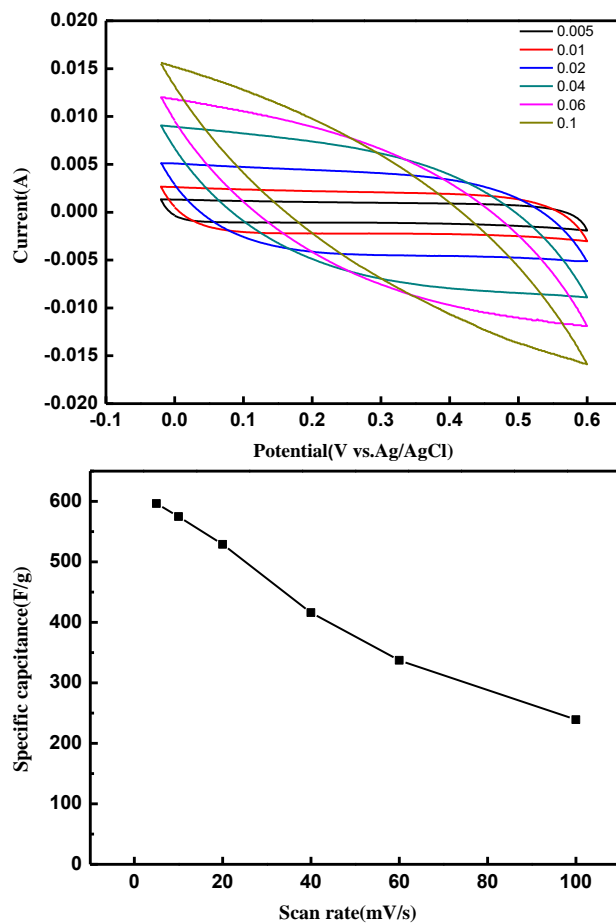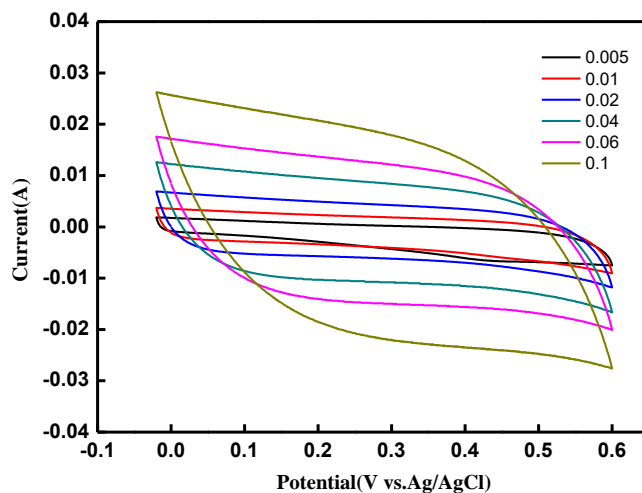
Figure 11. The cyclic voltammogram and capacitance at different sweep rates of C-PZs
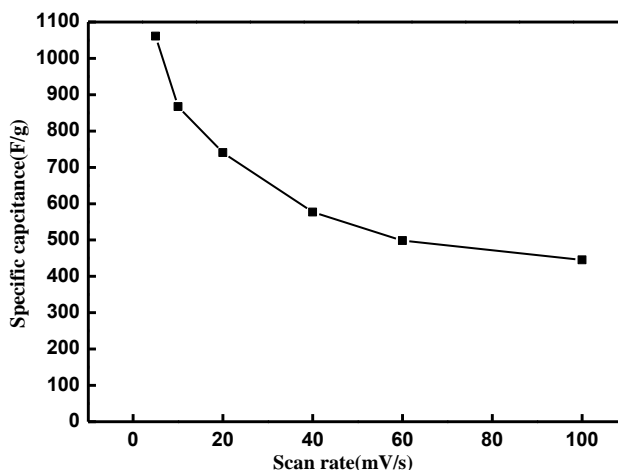
Figure 12. The cyclic voltammogram and capacitance at different sweep rates of C-PZs@CoS$_2$

By comparing the curves between different samples, it can be seen that the PZs microspheres coated CoS$_2$ have larger capacitance than pure PZs microspheres, which indicates that the PZs microspheres coated CoS$_2$ have better electrical properties. However, the specific capacitance of the C-PZs@CoS$_2$ decreases significantly, indicating that the stability of the materials are not particularly excellent.

4. CONCLUSIONS

Using the induced self-assembly properties of polyphosphonitrile template coated CoS$_2$ to form PZs@CoS$_2$ composite microspheres as carbon source by high temperature carbonization to prepare of porous carbon materials. Porous carbon materials channel make CoS$_2$ embedded with lithium ions can still contact process in order to obtain high lithium storage capacity. The structure of the porous carbon can avoid CoS$_2$ volume change which caused by performance degradation at the same time. In addition, PZs can be used as microspheres carbon source to obtain larger contact area and further optimize the electrochemical performance. The experimental results confirmed the rationality of the synthetic idea. Therefore, the use of polyphosphonitrile as carbon source for the preparation of composite sulfur materials has a great prospect in the field of electrochemistry. It is believed that in the near future, polyphosphonitrile sulfur composite materials will be widely used and bringing benefits to human beings after continuous optimization of the synthetic process and further modification.

References

1. U. Tunca, A. Erdogmus and G. Hizal. *Polym. Sci. Part A, Polym. Chem.*, 39 (2001) 2993.

2. E. C. Kellam, M. A. Hofmann and H. R. Allcock. *Macromolecules*, 34 (2001) 5140.
3. D. A. Stone, Y. Chang and H. R. Allcock. *Polym. Sci. Part A, Polym. Chem.,* 44 (2006) 69.
4. Z. Z. Zhao, Z. Z. Zhou, J. B. Ji and F. Xie, *Int. J. Electrochem. Sci.*, 10 (2015) 4303.
5. T. Zhang, Q. Cai, D. Wu and R. Jin. *Appl. Polym. Sci.*, 95 (2005) 880.
6. J. Fu and Q. Xu. *Adv. Mater. Res.*, 266 (2011) 188.
7. J. Fu, Y. Huang, Y. Pan, Y. Zhu, X. Huang and X. Tang. *Mater. Lett.*, 62 (2008) 4130.
8. J. Fu, Z. Chen, Q. Xu, J. Chen, X. Huang and X. Tang. *Carbon*, 49 (2011) 1037.
9. P. Gao, J. Fu, J. Yang, R. Lv, J. Wang, Y. Nuli and X. Tang. *Phys. Chem. Chem. Phys.*, 11 (2009) 11101.
10. Y. Li, Z. Zhou and S. Zhang, *J. Ame. Chem. Soc.*, 130 (2008) 16739.
11. C. Feng, J. Ma and H. Li, *Mater. Res. Bull.*, 44 (2009) 1811.
12. H. Li, W. Li, L. Ma, W. Chen and J. Wang, *J. Alloy. Compd.*, 471 (2009) 442.
13. H. S. S. Matte Ramakrishna, A. Gomathi and A. K. Manna, *Angewandte Chemie*, 122 (2010) 4153.
14. K. Chang, W.X. Chen and L. Ma, *J. Mat. Chem.*, 21 (2011) 6251.
15. F. Li, W. J. Liu, K. H. Li, W. Y. Chen, D. H. Xu, X. Y. Yu and H. Hu, *J. Electroanal. Chem.*, 824 (2018) 67.
16. C. Li, M. Zhao, C. N. Sun, B. Jin, C. C. Yang and Q. Jiang, *J. Power Sources*, 397 (2018) 162.
17. Q. H. Tian and W. Zhang, *Mater. Lett.*, 190 (2017) 177.
18. Z.P. Zhao, Z.P. Zhou and M. Q. Zhong. *Int. J. Electrochem. Sci.*, 12 (2014) 8120.
19. H. Li, W. Li, L. Ma, W. Chen and J. Wang. *J Alloy Compd*, 471 (2009) 442.
20. X. Q. Xie, S. J. Wang, K. Kretschmer and G. X. Wang, *J. Colloid Interf. Sci.*, 499 (2017) 17.
21. Z. W. He, J. Yang and Q. F. Lu. *ACS Sustain Chem Eng*, 1 (2013) 334.
22. M. M. Ren, M. Z. Yang, W. L. Liu, M. Li and H. Y. Ma, *Electrochim. Acta*, 194 (2016) 219.
23. Amir H. Farokh Niaei, Tanveer Hussain, Marlies Hankel and Debra J. Searles, *J. Power Sources*, 343 (2017) 354.